Measurement of the Partial Molar Volume and Solubility of Hydrogen in its Dilute Solutions in Palladium–Silver Alloys[1]

W. T. Lindsay, Jr.[2]

Linear expansion of thin-wall tubes of palladium–silver alloys containing 10, 20, 27, and 40 wt% silver was measured on absorption of small amounts of hydrogen (hydrogen-to-metal atom ratio, 0.005 to 0.25) at temperatures between 150°C (423 K) and 350°C (623 K) for equilibration with gaseous hydrogen at pressures up to around 1 bar. Hydrogen uptake by the test specimens was determined concurrently with the expansion measurements. Thermal expansion coefficients for the hydrogen-free materials were also obtained. Analysis of the data indicates that fractional length change is linearly dependent on hydrogen-to-metal atom ratio within the experimental range of hydrogen concentrations, independent of temperature, and varies only slightly with alloy composition. Partial molar volumes of hydrogen (with 95% confidence limits) vary from $1.77 \pm 0.08 \mathrm{cm}^3 \cdot (\mathrm{mol\ H})^{-1}$ for the 10% Ag alloy to $1.92 \pm 0.03 \mathrm{cm}^3 \cdot (\mathrm{mol\ H})^{-1}$ for the 40% Ag alloy. Hydrogen solubility results are correlated by a relation that facilitates linear extrapolation for determination of limiting values for equilibrium constants. Heats of solution of hydrogen at infinite dilution and standard entropy changes are essentially independent of temperature within the range of experimental conditions.

KEY WORDS: expansion; hydrogen; palladium–silver alloys; partial molar volume; solubility; thermal expansion coefficient.

1. INTRODUCTION

Expansion of the metal lattice when hydrogen is absorbed by palladium and its alloys is a striking effect that has long been recognized as an important factor in the thermodynamics of the solution process. Most investigations of this phenomenon have been by X-ray diffraction methods, with

determination of lattice parameter changes on substantial change of hydrogen content, most notably the difference in lattice parameters for coexisting α and β phases. There have been a few mechanical measurements of expansion [1–3]. Only Feenstra et al. [3] included low concentrations of hydrogen in their measurements with pure palladium, but they do not claim accuracy for hydrogen-to-metal atom ratios less than 0.04. This paper reports the results of precision dilatometric measurements of the expansion of palladium–silver alloys on absorption of measured small amounts of hydrogen (hydrogen-to-metal atom ratio 0.005 to 0.25).

2. EXPERIMENTS

2.1. Materials and Apparatus

The measurements were made on palladium–silver alloy tubes 9 in. (228.6 mm) long $\times \frac{3}{16}$ in. (4.76 mm) in diameter $\times 0.002$ in. (0.05 mm) in wall thickness. The tubes were obtained from Bishop and Company, Malvern, PA, with the following compositions: 90% Pd 10% Ag, 80% Pd 20% Ag, 73% Pd 27% Ag, and 60% Pd 40% Ag (compositions stated as weight percentage). Short stainless-steel end pieces, with radial holes to allow access of gas to the tube interior, were spotwelded to the ends of the tubes. The effective lengths of the tubes between spot welds were measured with a Cambridge Universal measuring machine.

Figure 1 is a photograph of the apparatus, which consisted essentially of a vacuum and gas manifold system connected to a length of stainless-steel tubing (the "furnace tube"), $\frac{3}{8}$ in. (9.53 mm) o.d. $\times \frac{1}{4}$ in. (6.35 mm) i.d., passing vertically through a center hole in an aluminum cylinder (the "furnace") approximately 18 in. (457 mm) long $\times$ 4 in. (102 mm) in diameter. The furnace was electrically heated by contoured strip heaters covering its cylindrical surface. Circulator guard heaters were attached to the upper and lower surfaces. The heaters were regulated to maintain an isothermal and constant temperature zone approximately 12 in. (305 mm) long centered within the aluminum cylinder. Temperatures were measured at several elevations by thermocouples.

Within the furnace tube, the test specimen was suspended in the center of the isothermal zone by a small-diameter stainless-steel rod that was threaded into the specimen's upper end piece and connected to a reference point located above the furnace. A similar stainless-steel rod, threaded into the lower end piece, suspended the magnetic core for a linear variable differential transformer (LVDT), Schaevitz Type 033SS-LT, 1000 cps, within the furnace tube at a location below the furnace. The transformer coil unit
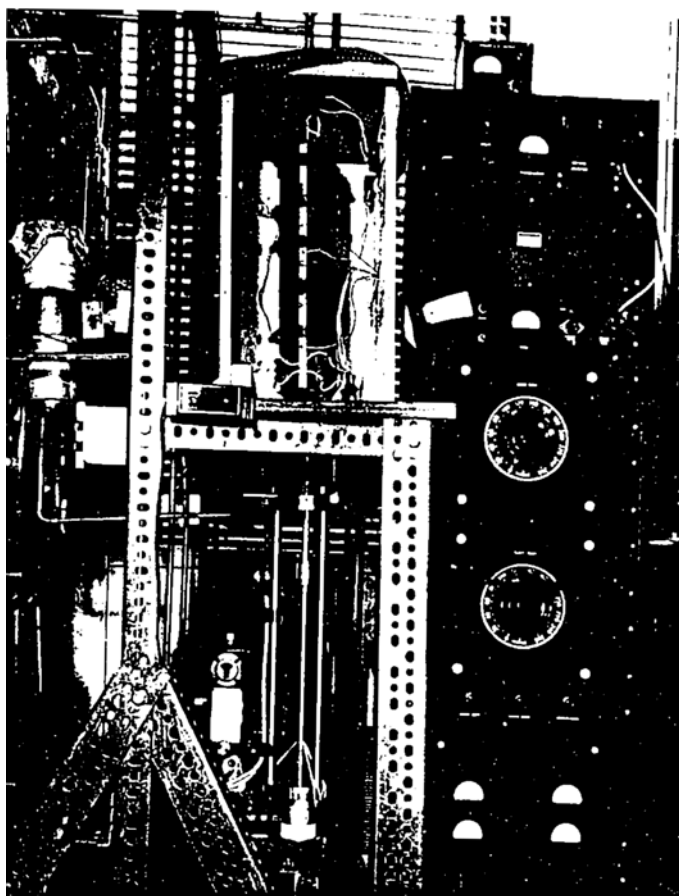
Fig. 1. Experimental apparatus. The furnace is at the top, with insulation removed to show heaters and thermocouples. LVDT transformer coils and micrometer system are visible on the furnace tube extending below the furnace.

for the LVDT was mounted on the outside of the lower extension of the furnace tube, supported by a stainless-steel sleeve sliding on the outside of the furnace tube and held firmly against the support sleeve by a weight riding above the transformer. Vertical movement of this assembly was effected by a precision micrometer mounted at the end of the furnace tube extension. All stainless-steel parts were AISI Type 304.

The concentric arrangement for suspension of the test specimen and the LVDT core assured that movement of the LVDT magnetic core relative to the position of the external transformer coils would not be

affected by unwanted differential expansion effects. Temperature differences between the furnace tube and the parts within it were effectively eliminated by the presence of either helium or hydrogen gas when measurements were made. Consequently, all changes in relative position of the LVDT magnetic core and the external transformer coils could be assigned to changes in length of the specimen tube relative to the furnace tube within the isothermal zone of the furnace.

Movement of the LVDT core within the lower extension of the furnace tube was measured by shift of the null signal position of the transformer coils. A 1000-cps signal generator, amplifier, tuned filter, and oscilloscope detector were used for null point detection. Precision of location of the null point was better than $\pm 1 \mu$m and was limited by ability to read the micrometer.

The vacuum and gas manifold assembly was connected to the upper extension of the furnace tube via a cold trap. The manifold assembly included provisions for evacuating the system and for admission of either helium or hydrogen gas. Isolating valves were provided to allow hydrogen uptake and pressure equilibration to be monitored. Gas pressures were measured with a mercury manometer. A container of known volume was connected to the system for volumetric calibration of the isolated section that included the furnace tube and its test specimen, thus allowing the quantity of hydrogen taken up by the specimen to be measured.

2.2. Procedure

The experimental procedure consisted of first determining a reference null point position for the LVDT coil unit when the hydrogen-free test specimen was equilibrated at furnace temperature while helium gas was present in the furnace tube. Then, at a constant furnace temperature, the helium was pumped out and replaced with a known volume of hydrogen. The change in length of the test specimen was monitored as equilibration with hydrogen took place. Following equilibration, final hydrogen gas pressure was measured, hydrogen uptake by the specimen was determined by the volumetric apparatus which had previously been calibrated with helium, and the final length increase of the specimen was recorded. Each test sequence consisted of one to three doses of hydrogen, with length change, pressure, and uptake measurements after each dose. Then the hydrogen was evacuated from both the apparatus and the specimen, and the "helium zero" reference position of the LVDT coil null point was redetermined. Reproducibility of the helium zero reference position was excellent, indicating no measurable hysteresis at the hydrogen concentrations of these experiments. The entire procedure was repeated several times at

each of several temperatures for each test specimen. The temperature range was from 150 to 350°C. Below 150°C, equilibrium could not be obtained in times short enough to allow the desired number of measurements.

Thermal expansion data for the test materials were determined from the change of helium zero (hydrogen-free) micrometer readings with temperature. This was a direct measure of differential thermal expansion of the specimen vs AISI Type 304 stainless steel.

3. RESULTS

3.1. Experimental Results

Figure 2 shows most of the measurement results on a plot of fractional length change as a function of experimentally determined hydrogen-to-metal atom ratio. The linear relationship between fractional length change and hydrogen content appears to be little affected by either temperature or composition of the metallic phase. This subject was examined statistically by comparing standard deviations of constants obtained by linear least-squares treatment of appropriate subsets of the data. For a given metallic composition, there is no significant variation with either temperature or hydrogen concentration, within the range of experimental conditions. However, there is a small systematic change with alloy composition.
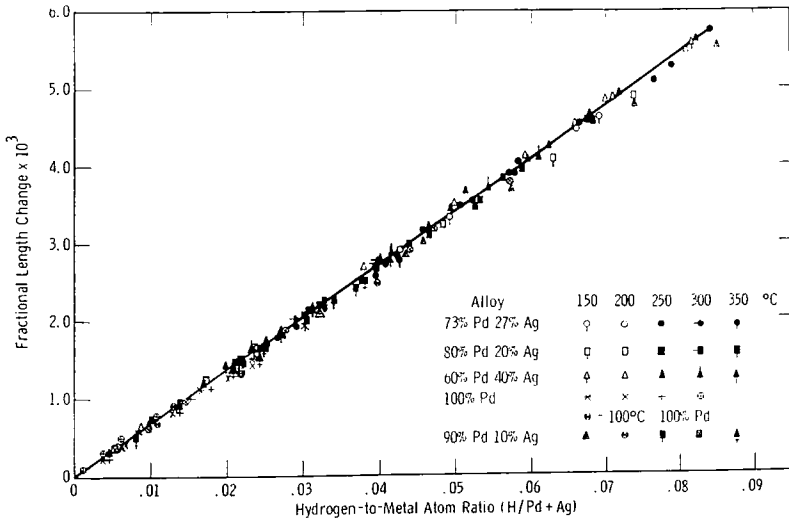
Fig. 2. Composite plot for all materials and temperatures, showing fractional length change as a function of experimentally determined hydrogen concentration. Some unpublished results for pure palladium are included for comparison.

Table I. Experimental Results

(A) Hydrogen expansion coefficients Γ for palladium–silver alloys

Alloy composition (wt%)	Temp. range (°C)	Conc. range $[n_H \cdot (n_{Pd} + n_{Ag})^{-1}]$	Mean value of Γ	SD	No. of runs
90 Pd 10 Ag	150–350	0.005 0.094	0.0655	±0.0014	37
80 Pd 20 Ag	150 350	0.014 0.204	0.0652	±0.0004	29
73 Pd 27 Ag	150 350	0.014 0.241	0.0661	±0.0008	45
60 Pd 40 Ag	150 350	0.006–0.142	0.0681	±0.0006	40

(B) Thermal expansion coefficients α for palladium–silver alloys

Alloy composition (wt%)	Temperature range of data (°C)	Mean value of α, 150–350°C[a] (10^6 K^{-1})
90 Pd 10 Ag	25–350	12.8
80 Pd 20 Ag	25–400	13.3
73 Pd 27 Ag	30 350	13.5
60 Pd 40 Ag	25–350	14.0

[a] Temperature range of hydrogen solubility and length change measurements.

The slopes of the least-squares lines for data at a given composition are hydrogen expansion coefficients, Γ, defined as

$$\Gamma = \Delta l/ml_0 \tag{1}$$

in which Δl is length change, l_0 is the reference length of the hydrogen-free specimen, and m is the hydrogen-to-metal atom ratio, $n_H/(n_{Pd} + n_{Ag})$. Table IA gives mean values of Γ for the series of alloys.

Table IB gives the results of thermal expansion measurements on the hydrogen-free specimens. Thermal expansion coefficients were calculated on the basis of a mean value of $17.8 \times 10^{-6} \text{ K}^{-1}$ for the thermal expansion coefficient of AISI Type 304 stainless steel in the temperature range of these measurements.

3.2. Derived Results

Partial molar volumes for hydrogen were calculated from the hydrogen expansion coefficients given in Table I according to

$$\bar{V}_H^0 = 3\Gamma[xV_{Pd} + (1 - x) V_{Ag}] \tag{2}$$

Table II. Derived Results

	Alloy composition			
	90% Pd, 10% Ag	80% Pd, 20% Ag	73% Pd, 27% Ag	60% Pd, 40% Ag
(A) $-\log K_0 = \Delta G^0 \, 2.30259 \, RT \pm SD$ (units of K_0, bars$^{-1\,2}$)				
Temperature (°C)				
150	0.879	0.405	0.176	−0.281
	±0.003	±0.003	±0.017	±0.009
200	1.033	0.633	0.383	−0.039
	±0.000	±0.000	±0.007	±0.008
250	1.160	0.783	0.566	0.165
	±0.006	±0.008	±0.005	±0.004
300	1.254	0.919	0.712	0.367
	±0.003	±0.004	±0.007	±0.009
350	1.337	1.008	0.813	0.506
	±0.002	±0.008	±0.010	±0.013
(B) Partial molar volume, $\bar{V}_H^0$, standard enthalpy change, ΔH^0, and standard entropy change, ΔS^0, $\pm$ SD				
$\bar{V}_H^0$ [cm^3·(mol H)$^{-1}$]	1.77	1.79	1.83	1.92
	±0.04	±0.01	±0.02	±0.02
ΔH^0 [kJ·(mol H)$^{-1}$]	−11.70	−15.24	−16.30	−20.06
	±0.20	±0.49	±0.28	±0.44
ΔS^0 [J·(mol H)$^{-1}$ K^{-1}]	−44.45	−44.02	−41.90	−41.81
	±0.40	±0.96	±0.55	±0.87

where $\bar{V}_H^0$ is the hydrogen partial molar volume at infinite dilution, x is the atom fraction Pd in the hydrogen-free alloy, and V_{Pd} and V_{Ag} are the atomic volumes of pure Pd and Ag. Results for $\bar{V}_H^0$ are given in Table IIB.

The precision of hydrogen uptake measurements was considerably less than the precision of length change measurements in most of the runs. For the purpose of hydrogen solubility correlation, smoothed values for concentration of hydrogen in the alloys were calculated from length change measurements according to

$$m = \Delta l / \Gamma_m l_0 \tag{3}$$

where Γ_m is the mean value of the hydrogen expansion coefficient for each specific material composition. The smoothed solubility data were correlated satisfactorily by means of a simple expression:

$$\log[\, p^{1\,2}(m_p^0 - m_{Ag} - m)/m\,] = -\log K_0 + \beta m \tag{4}$$

where p is the measured hydrogen pressure, m is the hydrogen-to-metal atom ratio determined from Eq. (3), m_{Ag} is the silver-to-metal atom ratio in the alloy, m_p^0 is the effective number of holes per palladium atom in the d-band of pure Pd, K_0 is an equilibrium constant for the solution process in the limit of infinite dilution, and β is the coefficient for the first term in a power series expansion in m of the logarithm of the activity coefficient of dissolved hydrogen.

The value of m_p^0 was adjusted for linearization of plots of the left–hand side of Eq. (4) versus m. Satisfactory linearity for all alloy compositions at all temperatures was obtained with a common value of 0.56 ± 0.01 for m_p^0. Examples of linearized plots are shown in Fig. 3. Table IIA gives values of $-\log K_0$ obtained from the linearized plots by least-squares treatment of the data.

Parameters for the temperature dependence of $\log K_0$ were determined by linear least-squares fitting of $\log K_0$ as a function of $1/T$. Figure 4 shows that $\log K_0$ can be so represented accurately. Values of β, obtained from the data in plots such as Fig. 3, are much less regular in their variation with temperature. Although they show a general systematic trend (more negative values of β at lower temperatures), these results are not suitable
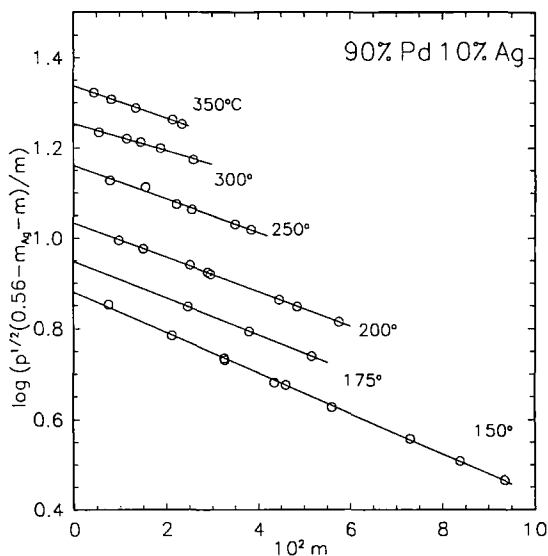

Fig. 3. Linear plots obtained for the 90% Pd/10% Ag alloy by application of Eq. (4) with m_p^0 set equal to 0.56. Similarly linear plots were obtained for the other alloys with the same value of m_p^0.
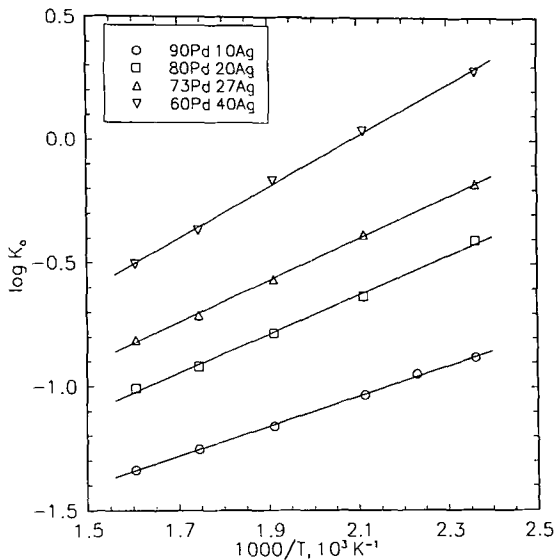
**Fig. 4.** Arrhenius plot of solubility constant at infinite dilution.

for representation as a function of temperature by an expression with a reasonable number of parameters. The mean value of β for all alloys and all temperatures is -3.19 (mol H)$^{-1}$, with a standard deviation of ± 0.60.

Standard enthalpy and entropy changes for the solution process were calculated from the data for $\log K_0$ as a function of temperature. The linear plots in Fig. 4 indicate that these enthalpy and entropy changes are essentially independent of temperature between 150°C and 350°C. Enthalpies of solution at infinite dilution and standard entropies of solution are given in Table IIB.

4. DISCUSSION

Partial molar volumes for hydrogen at infinite dilution in these alloys are not very different from values around 1.73 cm$^3 \cdot$ (mol H)$^{-1}$ obtained for hydrogen in the β phase of pure palladium from lattice parameter measurements by Owen and Jones [4]. Hydrogen in the β phase is known from neutron diffraction studies [5, 6] to occupy octahedral interstitial positions in the fcc metal lattice. The present results are consistent with the finding by Nelin [6] that hydrogen in the more dilute α phase also occupies octahedral interstices.

Equation (4) relates to equilibrium for a pseudo-chemical reaction assumed for the absorption process:

$$\tfrac{1}{2}H_2(g) + h_d(me) = H(me) \tag{6}$$
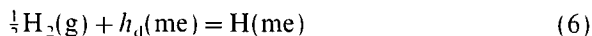
where h_d is a hole in the d-band of the alloy and (me) indicates the metallic phase. The reaction represented by Eq. (6) is supported by agreement of the value of 0.56 ± 0.01 for m_p^0, as derived from the solubility correlation, with a widely cited value of 0.55 for the number of holes per atom in the d-band of palladium [7]. In the formulation of Eq. (4), the standard state for dissolved hydrogen is taken to be a hypothetically ideal solution for which $m/(m_p^0 - m_{Ag}) = 1$. Derived thermodynamic quantitites correspond to use of this standard state.

All deviations from ideality are assigned to excess Gibbs free energy of hydrogen in its metallic phase solution. The linear plots illustrated in Fig. 3 indicate that this is a plausible assignment. The logarithm of activity coefficient for dissolved hydrogen varies as the first power of hydrogen concentration and the coefficients β are negative, implying short-range associative interaction between the dissolved entities. Such an implication is reasonable in view of theoretical suggestions, for example, Refs. 8 and 9.

Standard entropy changes for the solution process are nearly the same for all of the alloys. The enthalpies of solution at infinite dilution vary in a regular way that is related to the physical and mechanical properties of the alloys.

In conclusion, these measurements on dilute solutions have facilitated improved estimation of thermodynamic quantities for the H–Pd–Ag system.

ACKNOWLEDGMENTS

REFERENCES

1. T. Ooi, I. Ohno, and H. Numata, *Denki Kagaku oyobi Kogyo Butsuri Kagaku* 61:324 (1993).
2. E. S. Kodes, A. B. Zakharov, P. V. Gel'd, and N. I. Timofeev, *Izv. Vyssh. Uchebn. Zaved. Fiz.* 32:121 (1989).
3. R. Feenstra, R. Griessen, and D. G. DeGroot, *J. Phys. F. Met. Phys.* 16:1933 (1986).

4. E. A. Owen and J. I. Jones, *Proc. Phys. Soc. (London)* **49**:587 (1937); **49**:603 (1937).
5. J. E. Worsham, Jr., M. K. Wilkinson, and C. G. Shull, *J. Phys. Chem. Solids* **3**:303 (1957).
6. G. Nelin, *Phys. Status Solidi* **45**:527 (1971).
7. N. F. Mott and H. Jones, *The Theory and Properties of Metals and Alloys* (Dover, New York, 1958), pp. 199–200.
8. C. E. Buckley, J. F. Dobson, and M. A. Poyser, *J. Phys.: Condens. Matter* **7**:5815 (1995).
9. R. Burch, *Trans. Faraday Soc.* **66**:749 (1970).